



Enhancing sensorless control of SRM through instantaneous direct torque control with MGAO-CANN technique

Namala Ranjitkumar¹ · Kuthuri Narasimha Raju¹

Received: 22 February 2024 / Accepted: 6 April 2024

© The Author(s), under exclusive licence to Springer-Verlag GmbH Germany, part of Springer Nature 2024

Abstract

Switched reluctance motors (SRMs) have gained prominence in various industrial applications due to their robustness and simplicity. One critical aspect of enhancing SRM efficiency is precise control, often necessitating complex sensor systems for accurate feedback. This research addresses this challenge by proposing a sensorless control system based on instantaneous direct torque control (IDTC) techniques. The study introduces a novel architecture integrating a DC power supply, $(n + 1)$ diodes, and $(n + 1)$ switches, forming a foundation for SRM control without the need for additional sensors. The core innovation lies in the implementation of a modified genetic algorithm optimized cascaded artificial neural network (MGAO-CANN) controller. This controller refines control signals through genetic algorithm optimization and neural network computations, optimizing the motor's performance. To enhance system stability and prevent rapid fluctuations, a hysteresis current controller (HCC) is employed, ensuring smooth operation. The research's focal point is the application of instantaneous direct torque control, enabling real-time and precise adjustments to motor torque. By eliminating the necessity for extra sensors, the proposed system not only reduces costs significantly but also enhances SRM efficiency and responsiveness. The validation of proposed research simulated using MATLAB/Simulink and the outcomes reveals that the developed approach promises a ground breaking advancements in the realm of motor control technology.

Keywords Switched reluctance motors · MGAO-CANN · Instantaneous direct torque control · HCC · $(n + 1)$ diodes · And $(n + 1)$ switches

1 Introduction

Switched reluctance motors (SRMs) have emerged as preferred choices over traditional motors in specific applications in recent years, owing to advancements in power electronics and microelectronics technology [1]. The inherent simplicity of their mechanical structure simplifies the manufacturing process, reducing costs significantly [2]. Unlike conventional motors, SRMs feature rotors composed of iron stacks devoid of windings or magnets. This design enhances mechanical robustness, making them well-suited for high-speed operations. With a low moment of inertia and a high

torque-to-inertia ratio, SRMs deliver impressive torque levels at low-peak currents, utilizing small air gaps efficiently [3].

SRMs are favored for their low cost, simple structure, and environmental friendliness. They lack rare earth materials and operate in harsh environments, making them cost-effective and durable choices [4]. One major issue is the presence of large torque ripple, which occurs due to the nonlinear relationship between rotor position and electromagnetic torque. This fluctuation in torque output leads to vibrations and affects the motor's overall performance [5]. In high-speed applications, these vibrations become more pronounced, making it challenging to maintain stability and precision. Additionally, the torque ripple causes mechanical stress on the motor components, potentially leading to a shortened lifespan and increased maintenance requirements [6]. Research focused on torque ripple suppression holds significant engineering value because it addresses a critical issue in motor technology.

✉ Namala Ranjitkumar
ranjith.kumar110@gmail.com

Kuthuri Narasimha Raju
narasimharaju_eee@kluniversity.in

¹ Department of Electrical and Electronics Engineering, Koneru Lakshmaiah Education Foundation, Vaddeswaram, AP, India

One approach involves optimizing the motor design by strategically modifying its structure. This modification focuses on minimizing magnetic flux variations and enhancing symmetry within the motor, effectively reducing torque ripple [7]. However, achieving optimal modifications might require extensive analysis and testing, making it a time-consuming and resource-intensive process. Another avenue of research delves into sophisticated current control strategies [8, 9], such as hysteresis control and predictive algorithms. These techniques enable precise regulation of current flow, minimizing fluctuations in torque output, but computationally intensive, requiring powerful control hardware and software, which might increase system costs and complexity. Additionally, direct torque control (DTC) method [10] provides accurate control, but limits its real-time applicability in high-speed applications, where rapid processing is crucial. Similarly, integrating sensor feedback systems, utilizing sensors like encoders and resolvers, allows for accurate control of rotor position and current flow adjustments, ensuring a smoother torque output [11]. Besides, its merits of these sensors are susceptible to wear and require regular maintenance, leading to increased downtime and maintenance costs. Pulse width modulation (PWM) techniques [12–14] by finely tuning the current waveform through controlled voltage modulation in motor windings, PWM minimizes torque fluctuations. Despite, it leads to increased heat generation in motor, reducing overall efficiency.

Intelligent control methods, fuzzy logic [15] and neural networks [16], have emerged as powerful tools for real-time prediction and compensation of torque ripple. However, implementing these techniques requires more time to design and optimize. Overwhelming the limitations IDTC method [17, 18] stands out due to its ability to significantly reduce torque and flux ripples, ensuring a smoother motor operation. Compared to other control methods [19], IDTC offers a fast dynamic response, allowing the motor to promptly adapt to changing torque and flux demands. Moreover, algorithms are introduced in IDTC method to enable precise and real-time control of torque in SR motors. Table 1 demonstrates some of the existing algorithms introduced for torque control in SRM.

Addressing torque ripple suppression is crucial in current technological landscape, where industries are increasingly focused on optimizing performance, energy efficiency, and environmental impact. Solving this problem not only improves the functionality of existing applications but also opens up possibilities for development of new technologies and advancements in the field of electromechanical engineering. Therefore, research efforts directed toward torque ripple suppression to meet the demands of modern

engineering applications. The contributions of this research are as follows:

- Innovative sensorless control for SRMs, eliminating the need for external sensors.
- Designed an integrated setup using a DC power supply, diodes, and switches, simplifying SRM control mechanisms.
- Introduced a modified genetic algorithm optimized cascaded artificial neural network controller for real-time optimization of motor performance.
- Implemented a hysteresis current controller to ensure stable and smooth SRM operation, preventing rapid fluctuations.

2 Description of proposed system

The described system employs advanced control strategies, to enhance torque control and minimize torque ripple in SRM. This approach enables precise and efficient motor operation without the need for complex sensors, making it a promising advancement in motor control technology. Figure 1 demonstrates the proposed MGA-CANN-based IDTC approach. The input DC supply undergoes conversion using $(n + 1)$ diodes and $(n + 1)$ switches, facilitating the operation of the switched reluctance motor (SRM). This conversion process is fundamental for the motor's functionality. Voltage and current measurements from the motor serve as inputs for the back electromotive force (EMF) estimator. The estimated EMF data are then fed into a rotor position and speed estimator, where the difference between the reference speed and the actual speed (speed error) of SRM is calculated. This speed error is processed by a proportional-integral (PI) controller, generating a reference torque output. Simultaneously, the instantaneous total torque, computed from the torque estimator, is compared with the reference torque, yielding the torque tracking error. To address high torque ripple and achieve smooth torque control, a MGA-CANN controller is introduced. This controller refines the torque signals, improving precision. The resulting torque information is then sent to a reference current generator block, producing four reference phase currents (I_{aref} , I_{bref} , I_{cref} , I_{dref}). These currents, matching the magnitude of output from speed controller, are compared with the actual motor currents. Any disparities in current values are identified as current errors, which are input into HCC. The HCC processes these errors and generates necessary pulses for converter. These pulses are supplied to the SRM motor through a PWM generator implemented using FPGA Spartan 6E and a Driver Circuit (TLP250). This meticulous control strategy ensures precise modulation of current,

Table 1 Summary of existing algorithms in literatures

Authors/Year/Reference	Algorithm	Assessment	
Fahad Al-Amyal et al. (2023)/[20]	ACO	Objective	Utilizes optimized angles for implementing an improved DITC drive, focusing on reducing torque ripple and enhancing motor efficiency
		Limitation	Need for parameter tuning: ACO parameters need careful tuning for optimal performance, making it sensitive to settings
Renata Rezende C. Reis et al. (2023)/[21]	GA	Objective	GA to optimize commutation angles of SRM to reduce torque ripple
		Limitation	GA do not guarantee finding the global optimum
Kalai Selvi et al. (2023)/[22]	PSO	Objective	Optimize the performance of SRM
		Limitation	PSO converge to local optima, potentially missing the global optimum
Sydur Rahman et al. (2021) / [23]	GWO	Objective	Optimize SRM for EV application, aiming to enhance output torque density
		Limitation	GWO's convergence speed might vary based on the problem complexity
Nutan Saha et al. (2021) / [24]	MWOA	Objective	Optimize SRM for concurrent reduction of torque ripple and speed regulation
		Limitation	MWOA requires sophisticated implementation
Hossam Kotb et al. (2022) / [25]	LUS and SHO	Objective	Optimize cascaded PID controller for SRM to control speed and reduce torque ripples,
		Limitation	Algorithm performance depend on tuning parameters, requiring careful adjustment

allowing for smooth and efficient motor operation, marking a significant advancement in motor control technology.

3 Modeling of proposed system

3.1 Mathematical modeling of switched reluctance motor

SRMs is a type of electric motor that operates on the principle of magnetic reluctance. Unlike traditional electric motors, SRMs do not have a permanent magnet or a wound field on the rotor. Instead, the rotor consists of laminated iron cores,

and stator contains windings. An illustration in Fig. 2 depicts a typical cross-section of a four-phase 8/6 SRM. The motor operates by creating a magnetic flux path of least reluctance (magnetic resistance) between rotor and stator poles. When interphase coupling is ignored, the voltage across phase terminals of SRM is expressed as

$$v = Ri + \frac{d\phi}{dt} \quad (1)$$

The flux linkage ϕ in the context of stator winding resistance R considers the impact of both current and rotor

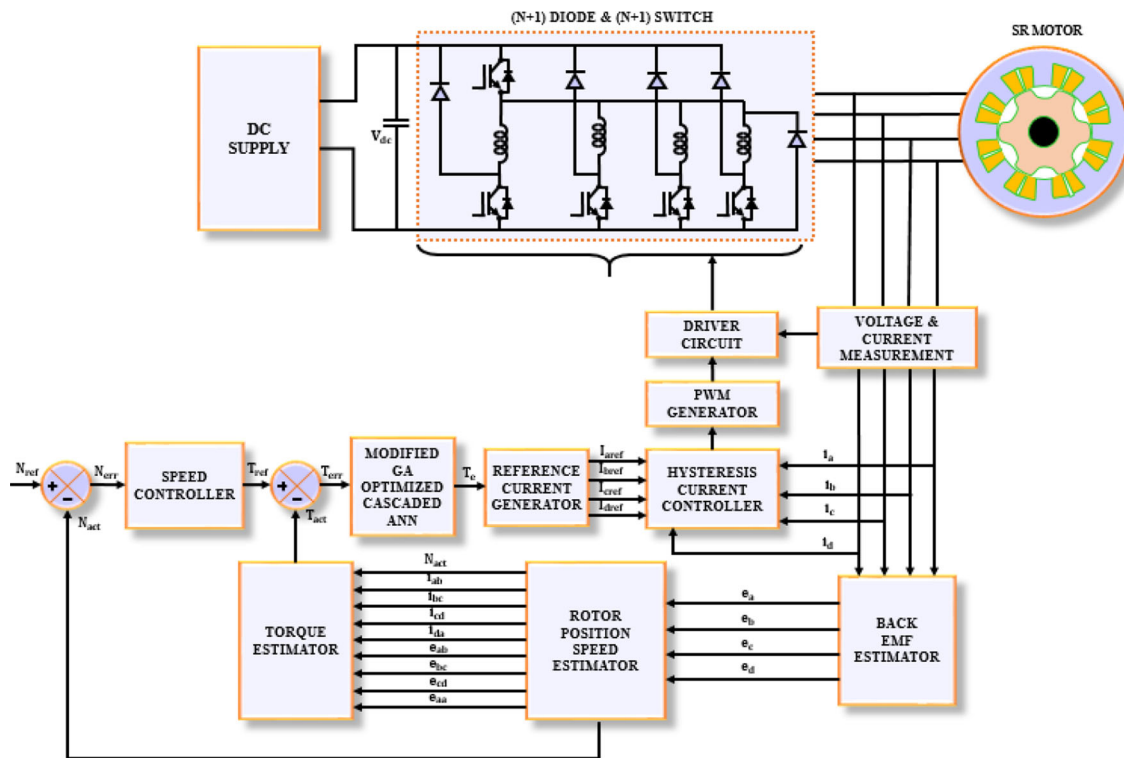


Fig. 1 Proposed system architecture

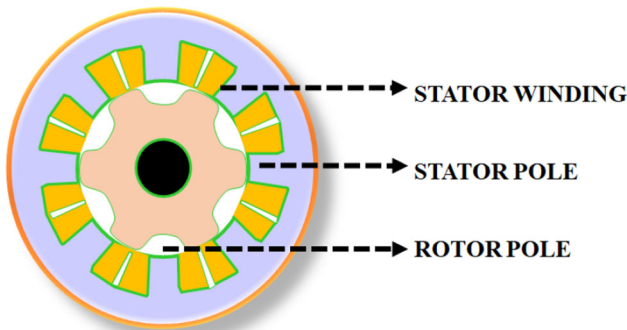


Fig. 2 Cross-section of four-phase SRM

position θ , allowing for the incorporation of magnetic saturation effects. In this scenario, flux linkage is defined as

$$\phi(\theta, i) = L(\theta, i)i(t) \tag{2}$$

The tangential force, leading to torque, arises from these factors. Given the sequential excitation in SRMs, both current and torque waveforms inherently exhibit pulsations [26].

SRMs exhibit two types of torque ripple: commutation torque (due to pulsed torque waveforms) and high-frequency torque (from switching actions). Commutation torque is

prevalent and related to inherent pulsations, while high-frequency torque arises from specific hardware and parameters. Tangential forces cause minor noise, but radial forces, significantly larger, are the main source of electromagnetic vibration and noise. Addressing these torque fluctuations and vibrations is crucial for wider SRM applications.

3.2 $n + 1$ Diode and $n + 1$ switch configuration

The use of $(n + 1)$ diode and $(n + 1)$ switch configuration in IDTC approach for SRMs involves the utilization of 'n' diodes and 'n' switches along with one additional diode and one additional switch. This configuration allows for precise control and optimization of SRM's performance, particularly in torque control and power conversion. In Fig. 3, a corresponding circuit is depicted, incorporating all the switching devices and diodes.

Each phase winding is powered from the DC supply when specific switches (S and S_1 for phase A, S and S_2 for phase B, S and S_3 for phase C, and S and S_4 for phase D) are closed, initiating motor operation. When phase A, accumulates energy, it is subsequently transferred back to the power source through diodes D_5 and D_1 after switches S and S_1 are opened.

Similarly, for phase B, energy stored during its activation is released back into the system via diodes D_5 and D_2 when switches S and S_2 are opened. Phase C and phase D operate in

Fig. 3 Configuration $n + 1$ diode and $n + 1$ switch converter

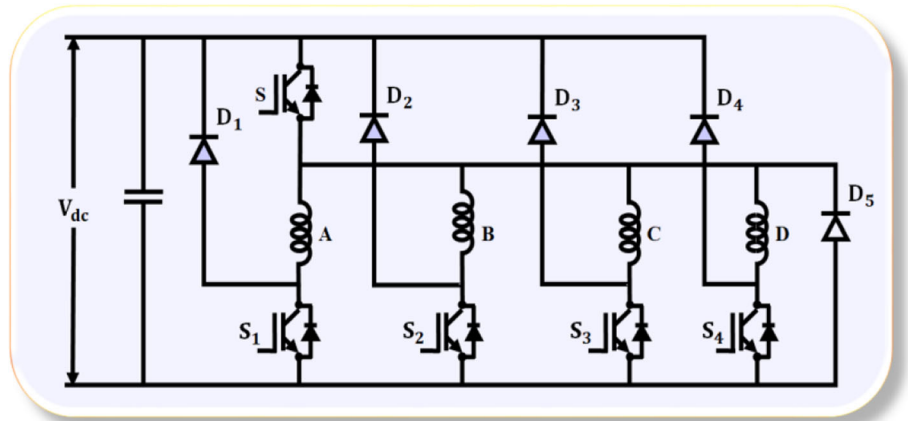


Fig. 4 Cascaded ANN for torque estimation

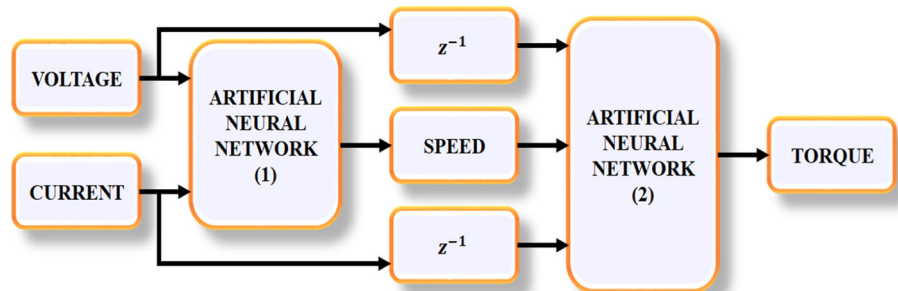
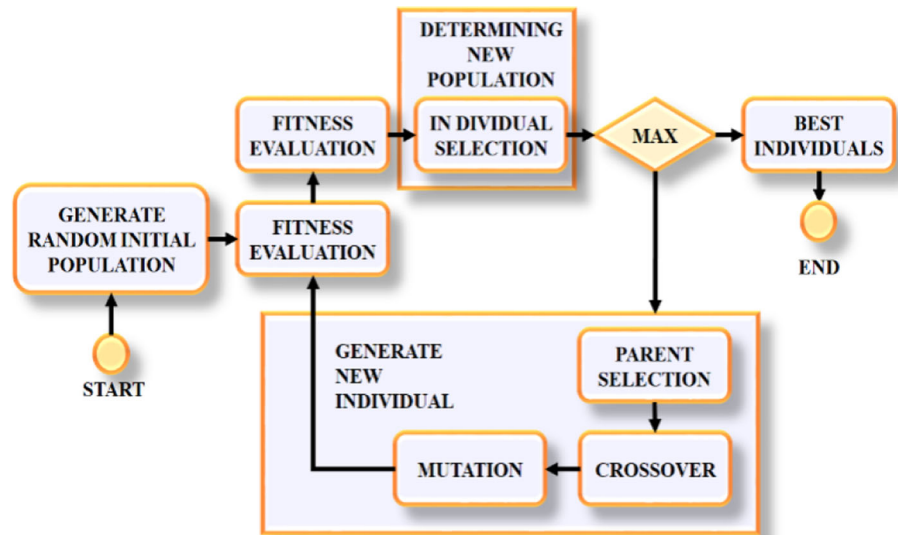


Fig. 5 MGA for torque control



a comparable manner, with energy returned to mains when switches S and S_3 and S and S_4 are opened. This system is designed to handle multiple phases (denoted as m) utilizing $(n + 1)$ power switches and $(n + 1)$ diodes for efficient control of current flow. The unique configuration ensures energy conservation and smooth operation by intelligently managing the release and utilization of stored energy in each phase.

The control strategy for the $(n + 1)$ diode and $(n + 1)$ switch configuration approach for SRM involves utilizing a

common switch S for all phases. This configuration simplifies the control system and to address the concern raised in the comment, the switching elements are controlled through a pulse width modulation (PWM) technique. PWM signals control the duty cycle of each switch, determining the duration for which each switch remains open or closed during a switching period. By adjusting the duty cycle of each PWM signal, the effective voltage applied to each phase winding

Table 2 Specification of MGA-CANN

Parameter	Rating
<i>Populationsize</i>	100
<i>No.ofgeneration</i>	50
<i>Crossoverprobability</i>	0.8
<i>Mutationprobability</i>	0.1
<i>Elitismrate</i>	0.1
<i>Fitnessfunction</i>	<i>MSEbetweenActualandestimatedTorque</i>
<i>Activationfunction</i>	<i>Sigmoid</i>
<i>Learningrate</i>	0.01

Table 3 Design parameter rating

Parameter	Ratings
<i>Numberofstator/rotorpoles</i>	8/6
<i>Ratedspeed</i>	3000r/min
<i>Nominalspeed</i>	315r/min
<i>Nominaltorque</i>	31Nm
<i>Maximumflux</i>	0.486WB
<i>Alignedinductance</i>	23.6mH
<i>Unalignedinductance</i>	5.9mH
<i>Statorresistance</i>	3.1Ω
<i>Saturatedalignedinductance</i>	0.15mH
<i>Maximumcurrent</i>	10A

is controlled, allowing for precise torque control and optimization of motor performance. The sequence in which the switches are turned on and off determines the direction of current flow in each phase winding. By appropriately sequencing the switches, the desired phase current profile is achieved, ensuring smooth motor operation and efficient power conversion. MGA-CANN adjusts the PWM signals applied to the switches based on the measured current, ensuring that the desired current profile is maintained and providing closed-loop control of the motor.

3.3 Torque control scheme of SRM motor

SRM, torque control plays a pivotal role in ensuring the motor which operates efficiently and accurately. SRMs are inherently robust and reliable, making them ideal for various industrial applications. However, their performance greatly depends on the precise regulation of torque output. Accurate torque control enables SRMs to respond dynamically to changing load demands. Furthermore, precise torque control is essential for maintaining stability and preventing mechanical stress within the motor components. By implementing

effective torque control strategies, it is possible to operate motor within safe limits, enhancing its longevity and reliability.

3.4 Cascaded ANN for torque control

The problem involves controlling torque output of SRM. To achieve this, a cascaded ANN structure is used, where multiple neural networks are arranged in sequence. The goal is to optimize the performance of these networks using a modified GA.

The proposed cascaded ANN operation for torque control is illustrated in Fig. 4. The first ANN is designed to estimate the speed of SRM based on two input parameters: RMS current ($X_{current}$) and RMS voltage ($X_{voltage}$) which is supplied to the motor. These parameters act as input to the input layer. Neurons in hidden layers perform computations using weights and biases, applying activation functions. The output layer computes the estimated speed (Y_{speed}) based on weighted sum of inputs and activations in hidden layers.

$$Y_{speed} = f_{speed}(w_{current}X_{current} + w_{voltage}X_{voltage} + b_{speed}) \quad (3)$$

where activation function is defined as $f_{speed}()$, weights associated with input voltage and current is specified as $w_{voltage}$ and $w_{current}$ and bias terms as b_{speed} . The network is trained using the input–output pairs followed by back propagation algorithm to adjust weights and biases iteratively, minimizing the difference between predicted and actual speed values.

The second artificial neural network estimates the torque demanded by the load. Its inputs include the speed estimated by the first network (Y_{speed}), ($X_{current}$) and ($X_{voltage}$). There is also a delay introduced to synchronize the data and ensure proper sequencing. The inputs (Y_{speed} , $X_{current}$, and $X_{voltage}$) are fed into the network. The inputs are synchronized with an appropriate delay to match the time instances when data are valid and relevant.

$$Y_{torque} = f_{torque} \left(w_{speed} Y_{speed} + w_{current} X_{current} + w_{voltage} X_{voltage} + b_{torque} \right) \quad (4)$$

where torque activation function is defined by f_{torque} , w_{speed} , $w_{voltage}$ and $w_{current}$ specifies the weights associated with speed, voltage and current and b_{torque} indicates bias term. Similar to first ANN, the network is trained using input–output pairs. Back propagation algorithm is employed to adjust the weights and biases, ensuring predicted torque values align closely with actual torque demands.

To optimize the performance of these cascaded neural networks for accurate torque control in SRM, modified GA is implemented.

3.5 Modified genetic algorithm

3.5.1 Fitness function

The fitness function serves as a measure of how well a particular set of neural network parameters (represented by chromosomes) perform the task of torque estimation. A lower fitness score indicates that the estimated torque values closely match the actual torque demands. Therefore, chromosomes with lower fitness scores represent solutions where the neural networks are accurately estimating the torque. The fitness function computes the difference between estimated and actual torque values for a given set of parameters. Lower differences result in lower fitness scores, indicating a better fit.

3.5.2 Chromosomes

In MGA, each chromosome contains the parameters of neural networks, including weights and biases. These parameters are encoded into the chromosomes, making them the genetic material that undergoes evolution.

3.5.3 Crossover and mutation

Crossover involves taking genetic information from two parent chromosomes and combining it to create offspring. This operation mimics the natural genetic recombination process and is essential for exploring different combinations of parameters while mutation introduces small random changes in genetic material of a chromosome. These changes encourage exploration of the solution space, preventing the optimization process from getting stuck in local optima.

3.5.4 Elitism

The best-performing individuals (chromosomes) from the current population and preserving them in next-generation without any changes. This strategy ensures that the best solutions are not lost and continue to contribute to the evolution process. Moreover, it maintains genetic diversity by retaining top solutions, preventing premature convergence of algorithm to suboptimal solutions.

3.6 Modified genetic algorithm optimized cascaded artificial neural network (MGA-CANN) controller

The MGA-CANN controller integrates the MGA optimization with cascaded neural network structure, forming a robust control system for applications like SRM torque control. Figure 5 illustrates the flow chart of MGA-CANN, and the specifications are listed in Table 2.

Objective function: The fitness function evaluates how well a particular set of parameters for the CANN system performs the task of torque estimation. It measures the accuracy of estimated torque values concerning actual torque demands. A lower fitness score indicates a better match between the estimated and actual torques.

Iterative Improvement: Through multiple generations, MGA explores various combinations of weights and biases for neural networks in CANN. By selecting, crossover, and mutating chromosomes over several iterations, the algorithm fine-tunes the parameters, aiming to minimize fitness score. This iterative process leads to the evolution of ANN configuration, enhancing its capability to estimate torque accurately.

Convergence: As the MGA progresses through generations, it converges toward sets of parameters for neural networks that result in minimal fitness scores. These parameters represent an optimized configuration for CANN.

These optimized parameters ensure that the neural networks accurately estimate the torque demanded by load based on input parameters, leading to precise torque control in SRM.

4 Results and discussion

In this section, the outcomes of the study, which were obtained through rigorous evaluation using MATLAB, are presented. Table 3 illustrates the parameter rating of proposed system. The findings provide valuable insights into the performance and effectiveness of proposed approach, shedding light on its practical implications and contributions to the field.

The proposed sensorless MATLAB simulink model for SRM is illustrated in Fig. 6. The model likely illustrates the integration of DC power supply, diodes, switches, and the

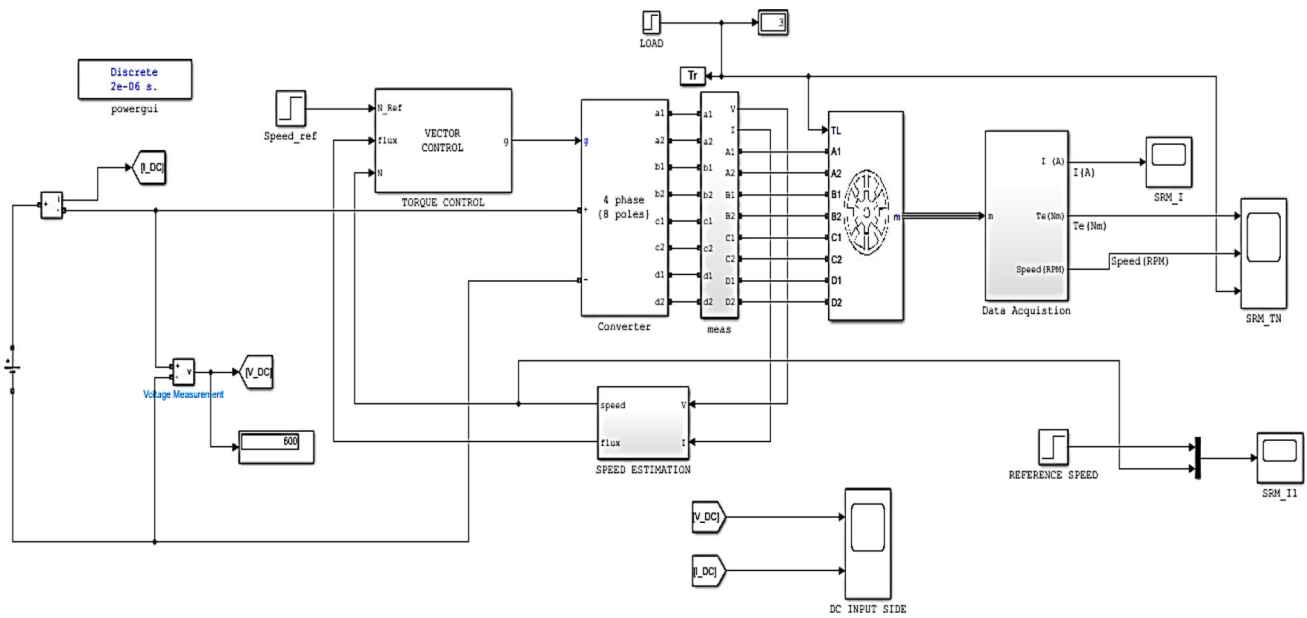


Fig. 6 MATLAB simulink model of proposed system

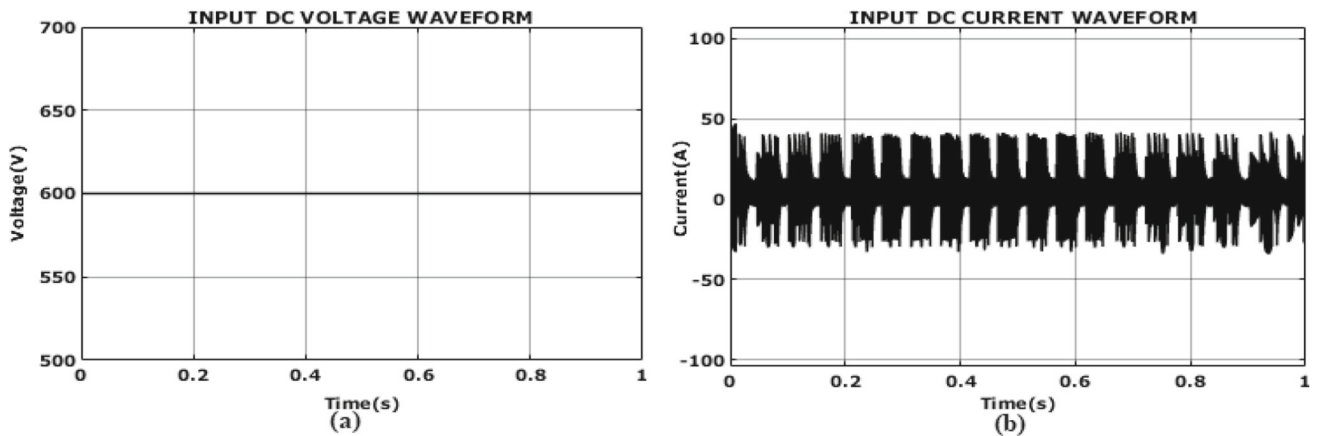


Fig. 7 Input DC: a Voltage and b current profiles

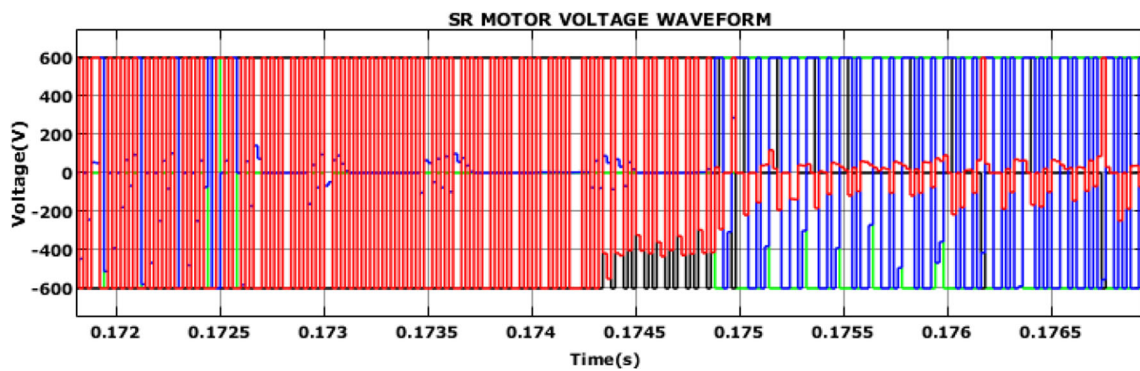


Fig. 8 SRM voltage waveform

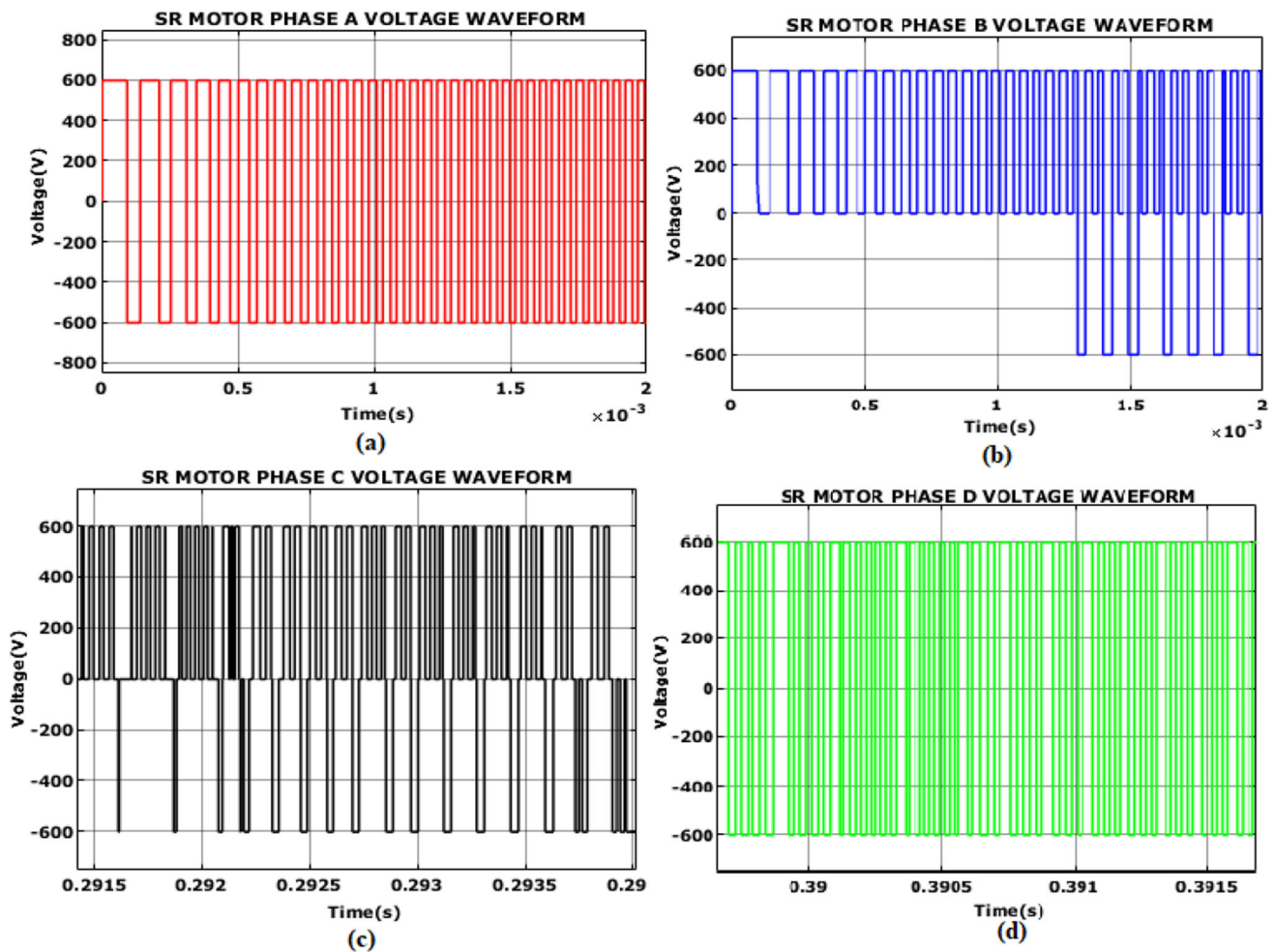


Fig. 9 Voltage characteristics of SRM: **a** Phase A, **b** phase B, **c** phase C, and **d** phase D

MGAO-CANN controller. This visual representation offers a concise overview of the system's architecture and the simulation setup, providing insights into the functional components of proposed research.

The description of Fig. 7 clarifies that the illustration captures the features of input power, displaying voltage and current waveforms attained at a speed of 1500 revolution per minute (r/min). Notably, it highlights a stabilized voltage of 600 V devoid of oscillations, followed by a corresponding current of 43 A. This information provides valuable insights into the consistent and controlled nature of input power for the proposed SRM.

An overview of SRM total voltage behavior is illustrated in Fig. 8. This waveform collectively represents the voltage across all phases of the motor, offering a comprehensive understanding of the system's electrical characteristics. The noteworthy observation is the consistent and stable voltage of 600 V achieved in this waveform. The absence of significant fluctuations or oscillations underscores the system's ability

to provide a steady and controlled electrical environment for the motor, which is essential for its efficient operation.

The voltage characteristics of SRM individual phases (A, B, C, and D) are detailed in Fig. 9. Each subplot (a, b, c, and d) likely represents the voltage waveform for a specific phase of the SRM. The critical observation here is the stability of the voltage at 600 V in each phase. It indicates that the proposed sensorless control system effectively maintains a consistent and controlled voltage supply to each phase of SRM. This stability is crucial for the reliable and optimal performance of the motor.

A detailed representation of current at individual phases (A, B, C, and D) of SRM is illustrated in Fig. 10. Each subplot (a, b, c, and d) likely corresponds to current waveform of a specific motor phase. The achievement of an average current value of 28A in each phase is a significant indicator of the stability and controlled operation of the SRM. This value reflects the balanced distribution of current across all motor phases, signifying that the proposed system effectively regulates the current flow.

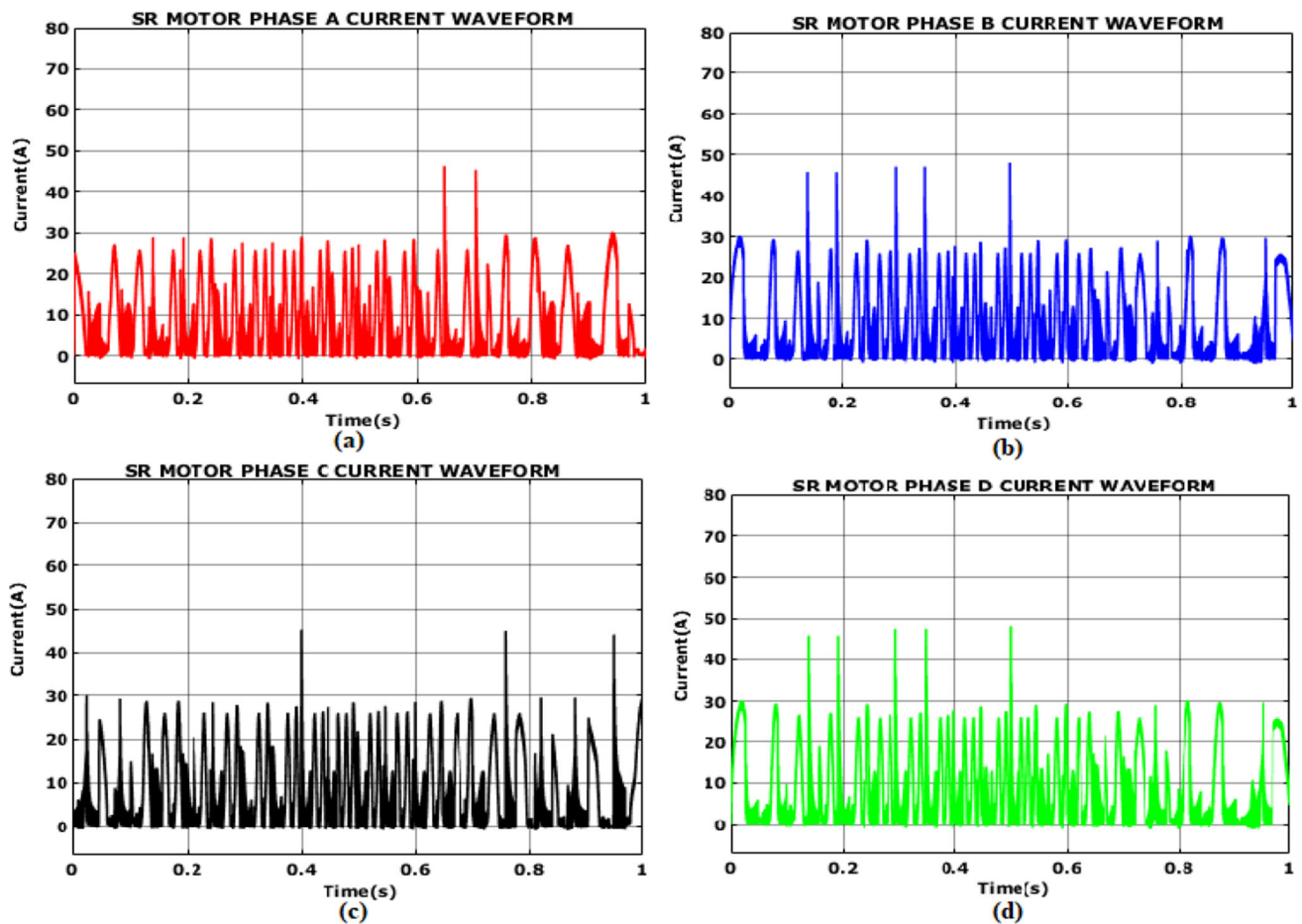


Fig. 10 Current characteristics of SRM: a Phase A, b phase B, c phase C, and d phase D

The magnetic flux characteristics of distinct phases (A, B, C, and D) within the SRM is delved in Fig. 11. Each subplot (a, b, c, and d) presumably outlines the flux waveform of a specific motor phase. Despite minor distortions, the figures reveal the attainment of a magnetic flux value of 0.4 WB. This shows that the proposed system effectively manages the magnetic flux, achieving a consistent and controlled flux level with only minor deviations.

4.1 At No load condition

The variation in system's speed when devoid of external load is illustrated in Fig. 12a, revealing initial fluctuations that eventually stabilize at 1500 r/min. The corresponding torque response is presented in Fig. 12b, showcasing initial variations aligning with the speed adjustments, followed by a stable torque maintenance at 8 N m. These figures collectively offer a comprehensive view of the system's dynamic behavior, emphasizing its ability to maintain steady-state operation in the absence of external loads.

4.1.1 At Load = 1 N m

The system's response to a 1 N m load condition is demonstrated in Fig. 13a illustrating the speed response and Fig. 13b depicting the torque behavior. Notably, the motor exhibits a tendency to maintain a constant speed of 1500 r/min despite the introduction of 1 N m load. The speed response shows minor variations during this load condition, suggesting the motor's ability to adapt and stabilize around the specified speed. Concurrently, the torque behavior in Fig. 13b reveals only slight fluctuations, settling at 7.6 N m. This indicates that the motor efficiently adjusts its torque output to counter the introduced load, demonstrating a stable and controlled response to applied 1 N m load condition.

4.1.2 At Load = 2 N m

In Fig. 14, the system's response to a 2 N m load condition is presented, with (a) depicting the speed variation and (b) illustrating the torque response. Notably, under 2 N m load, the motor maintains a consistent speed of 1500 r/min, indicating its ability to sustain the specified operating speed even in the

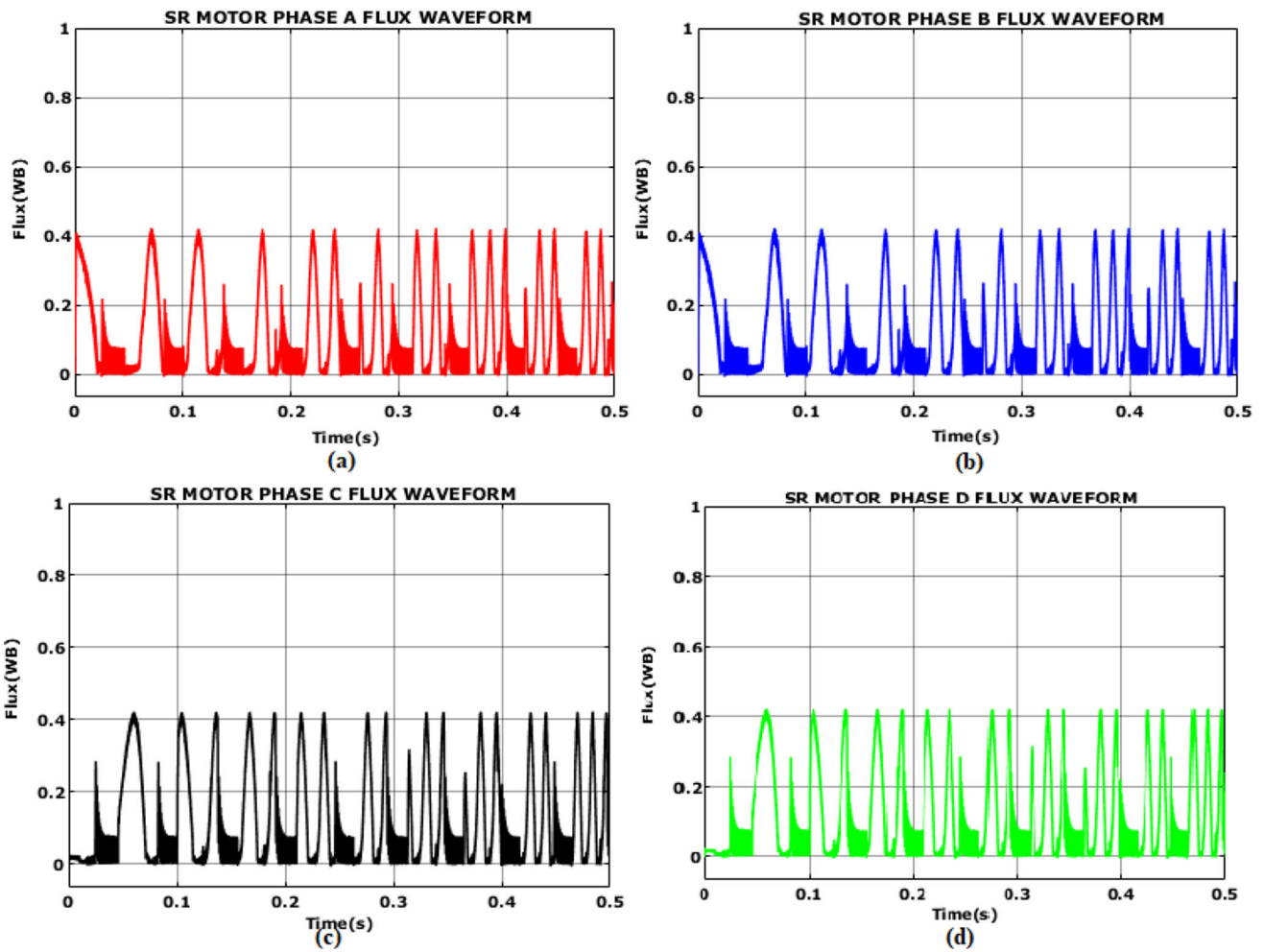


Fig. 11 Flux distribution in SRM: a Phase A, b phase B, c phase C, and d phase D

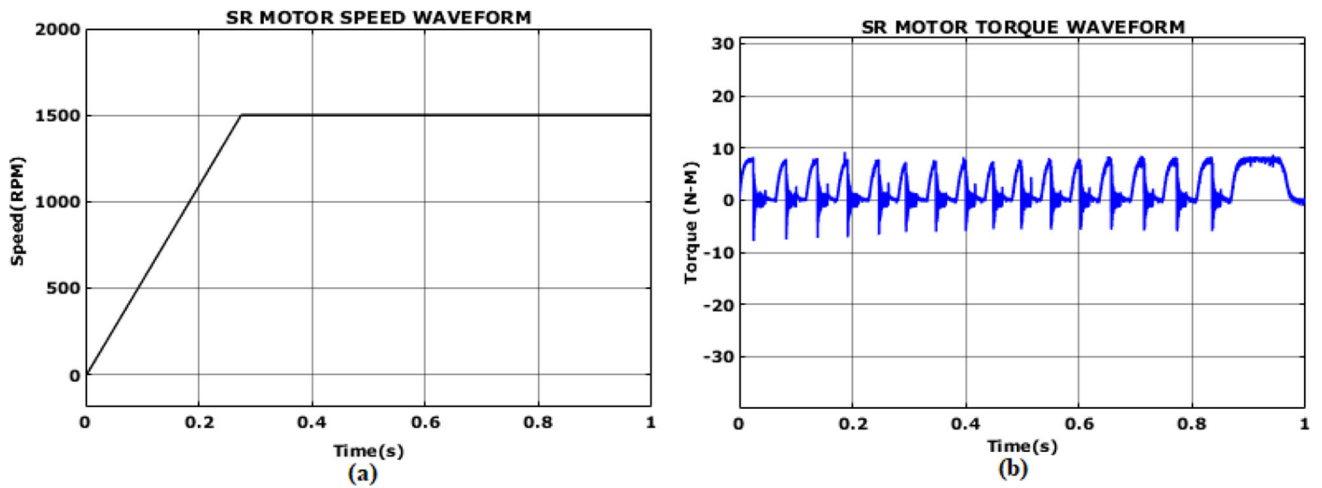


Fig. 12 a Speed variation and b torque profile under at no load condition

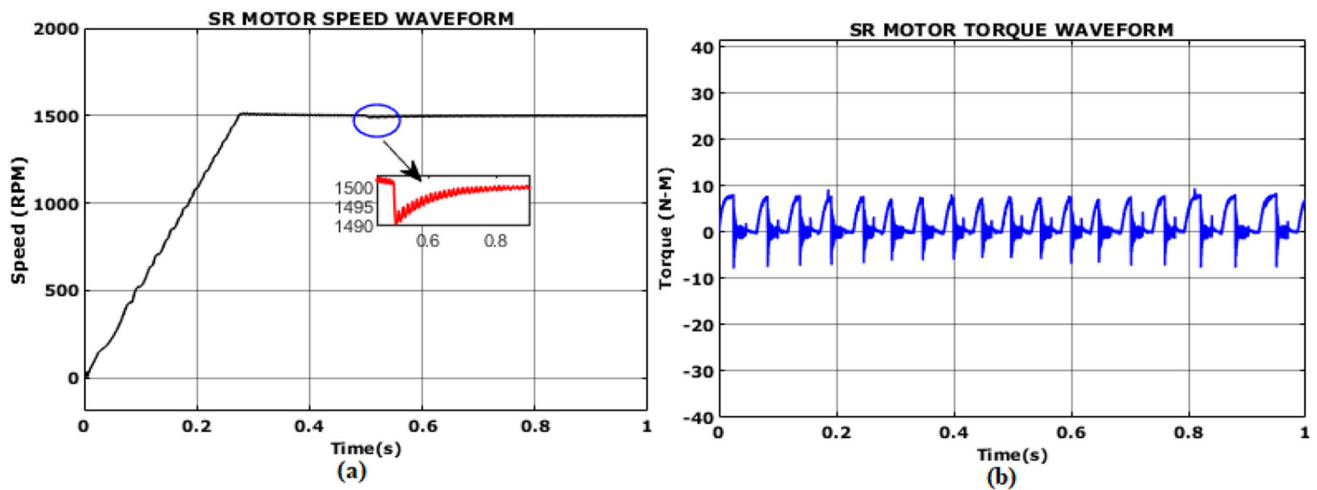


Fig. 13 a Speed response and b torque behavior under 1 N m load conditions

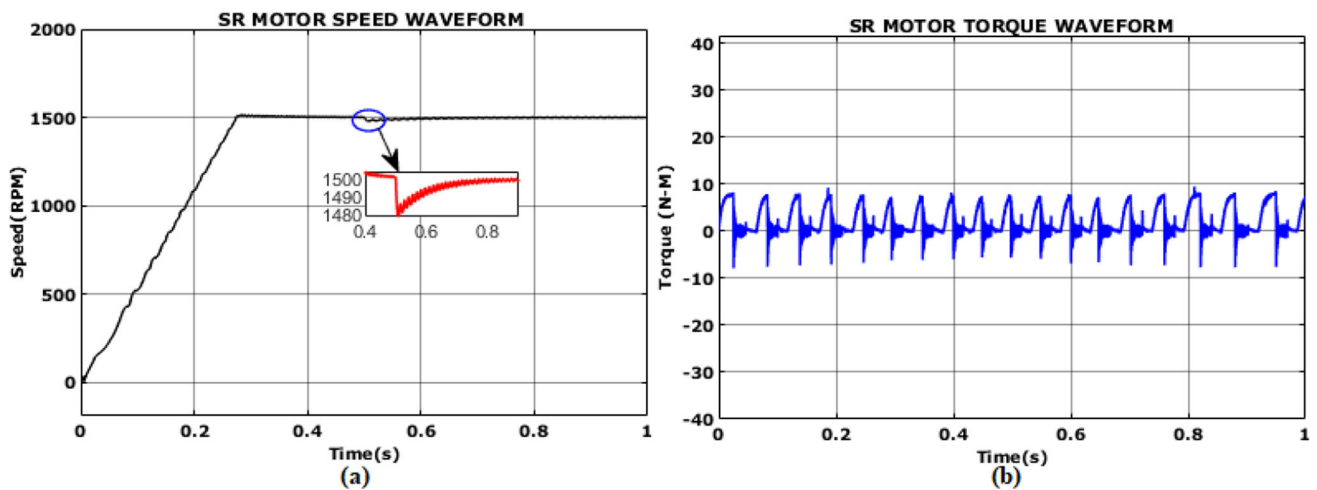


Fig. 14 a Speed variation and b torque response under 2 N m load condition

presence of increased load. A subtle change is observed in speed at 0.6 s, suggesting a transient response to load. In parallel, Fig. 14b shows the torque response, revealing a value of 7.9 N m. This torque value indicates the motor's ability to generate necessary torque to counter 2 N m load, reflecting a stable and controlled torque output. The synchronized information from both speed and torque responses provides valuable insights into the motor's performance under the specific 2 N m load condition, highlighting its adaptability and stability in maintaining operational parameters.

4.1.3 At Load = 3 N m

In Fig. 15, the system's behavior under a 3 N m load condition is illustrated, with (a) capturing the dynamics of speed and (b) representing the torque response. Notably, a gradual rise in speed is observed, suggesting an adjustment to the increased load. However, distortions become evident at 0.6 s, indicating

a transient response in the system. Despite these distortions, the speed tends to stabilize and maintain a consistent value of 1500 r/min. In response to variations in speed, Fig. 15b shows the torque response with minor fluctuations, settling around an average torque value of 7.9 N m. This suggests that motor effectively adapts to 3 N m load, demonstrating a stable speed response with corresponding minor variations in torque.

4.1.4 At varying loads

The depicted speed waveform of SRM in Fig. 16 showcases the motor's dynamic behavior. Initially, the speed rises from its starting level and stabilizes at 1500 r/min. Notably, at 0.5s, when a load is introduced, the speed gradually increases, reaching 2000 r/min and maintaining a constant level thereafter. This observation highlights the SRM's ability to adapt

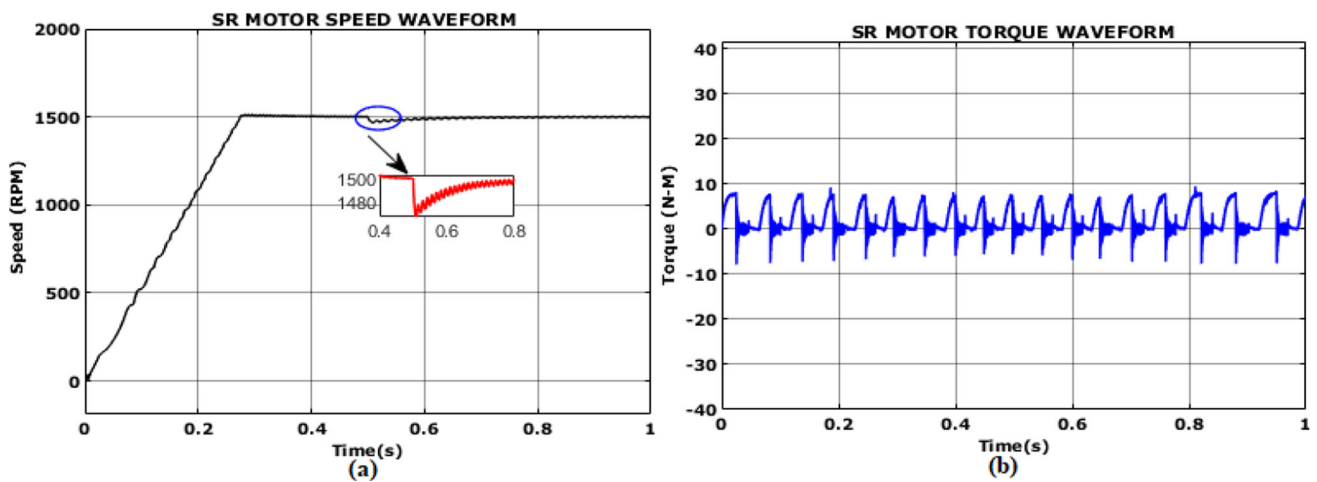


Fig. 15 a Speed dynamics and b torque response under 3 N m load condition

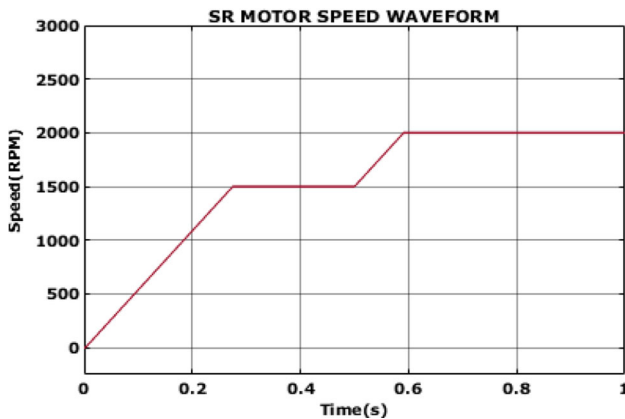


Fig. 16 SRM speed response under varying load

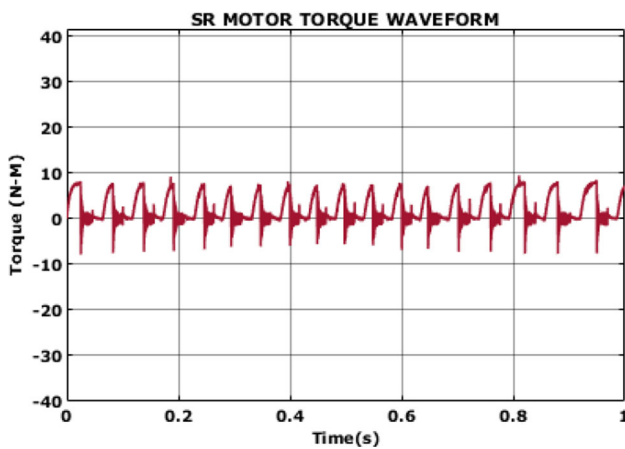


Fig. 17 Torque waveform of SRM

to varying mechanical loads, demonstrating a responsive and stable speed control mechanism.

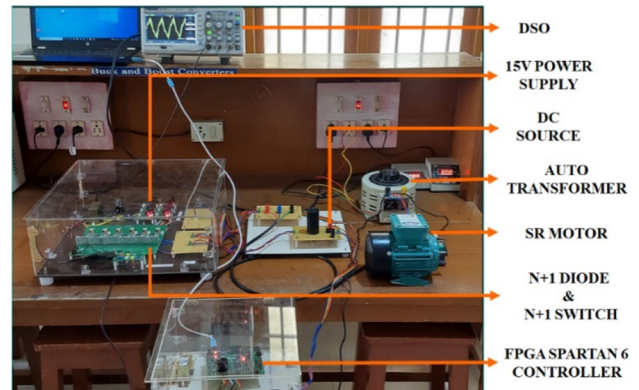


Fig. 18 Experimental prototype

The depicted Fig. 17 titled and provides an overview of the torque characteristics of SRM. Despite minor oscillations, the figure reveals the maintenance of an average torque value of 8 N m, utilizing MGA-CANN for torque control. The minor oscillations put forward a degree of responsiveness in torque control mechanism, demonstrating the system’s ability to adapt to dynamic conditions while sustaining an average torque level of 8 N m.

4.2 Hardware analysis

The experimental prototype as shown in Fig. 18 serves as a tangible demonstration of the research and validates the feasibility of proposed sensorless control system for SRM. The experimental setup includes FPGA controller programmed with MGA-CANN approach, HCC, and the SRM itself. Components such as power supplies, controllers, and motor connections are visible in the figure, contributes to a comprehensive understanding of the experimental setup’s complexity and functionality.

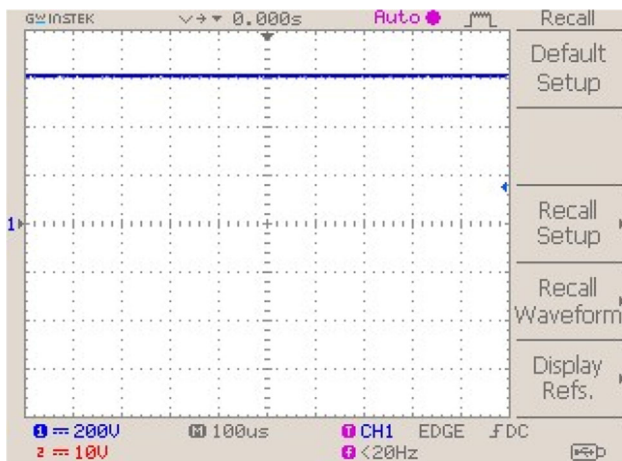


Fig. 19 Input DC voltage

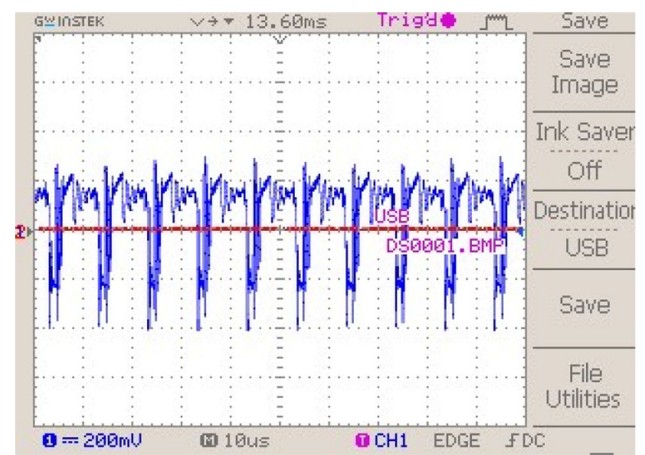


Fig. 21 SRM current dynamics waveform

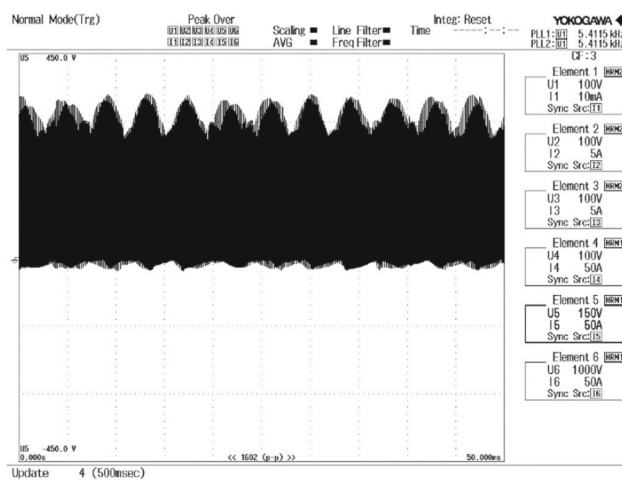


Fig. 20 SRM voltage waveform

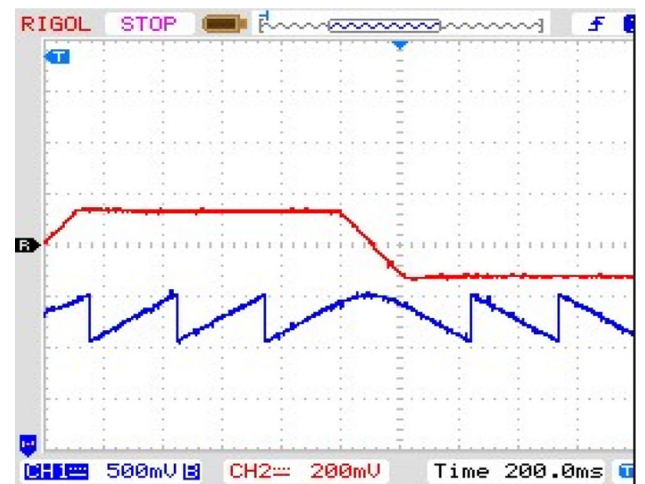


Fig. 22 Flux distribution in SRM

The input DC voltage waveform with a stable 600 V is a crucial aspect of SRM, as shown in Fig. 19. The stable 600 V input DC voltage serves as the power source for motor. This stability is essential for providing a consistent and controlled electrical environment to the SRM. A constant and stable input voltage ensures reliable and optimal operation of the motor, contributing to improved efficiency and responsiveness.

The voltage stability of SRM in all four is illustrated in Fig. 20, maintaining a consistent 600 V across the phases with minor oscillations. The observed minor oscillations indicate that the proposed sensorless control system manages the voltage waveform, ensuring that the SRM operates under controlled and stable electrical conditions.

The Fig. 21 captures the dynamic behavior of current flow through the motor's phases, offering insights into the responsiveness and efficiency of system. It is observed that an average current is obtained for efficient system performance

that is essential for understanding how electrical currents vary over time during the operation of the SRM.

Figure 22 presents a detailed illustration of the magnetic flux distribution in each SRM. This figure allows for a comprehensive examination of how the magnetic flux varies across different phases during the motor's operation. Analyzing the SRM flux at each phase contributes to a more thorough motor's magnetic behavior, aiding in the assessment of the control strategy's performance.

The torque waveform illustrated in Fig. 23 provides a detailed representation of the torque waveform generated by SRM during its operation. This figure illustrates how the torque output varies over time, indicating motor's performance and efficiency. The torque waveform aids and shows minimized torque owing to the proposed torque control strategy and contributes to a comprehensive understanding of the motor's behavior under the proposed control strategy.

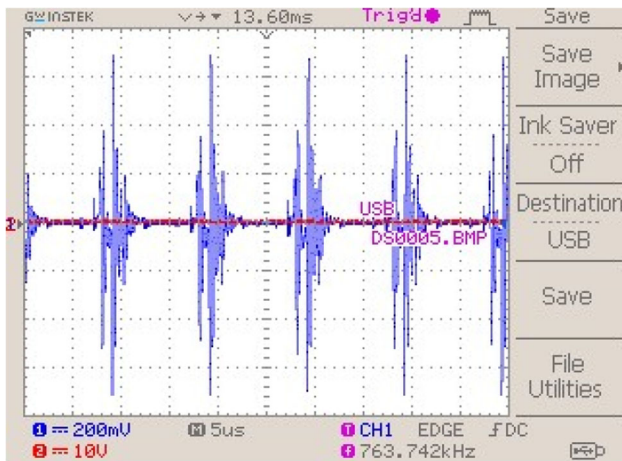


Fig. 23 Torque characteristics of SRM

Figure 24, visually represents the SRM speed waveform with minor oscillations, showcasing the motor’s ability to maintain a stable speed of 1500 r/min. A consistent and

Table 4 Comparison of torque ripple with different control approaches

Control techniques	Speed	Torque ripple (%)
ANN	2000	17.12
GA-ANN	2000	10.3
Proposed MGA-CANN	2000	5.2

controlled speed is achieved by the SRM, reflecting efficacy of implemented control strategy.

Table 4 compares the torque ripple achieved with different control approaches for a given speed of 2000 r/min. Torque ripple refers to the variation in torque output of a motor during operation, often undesirable as it can lead to vibrations, noise, and decreased performance in applications requiring precise torque control. The proposed MGA-CANN approach integrates multiple objectives and cooperative strategies within a genetic algorithm framework to optimize control parameters for reducing torque ripple. This advanced technique

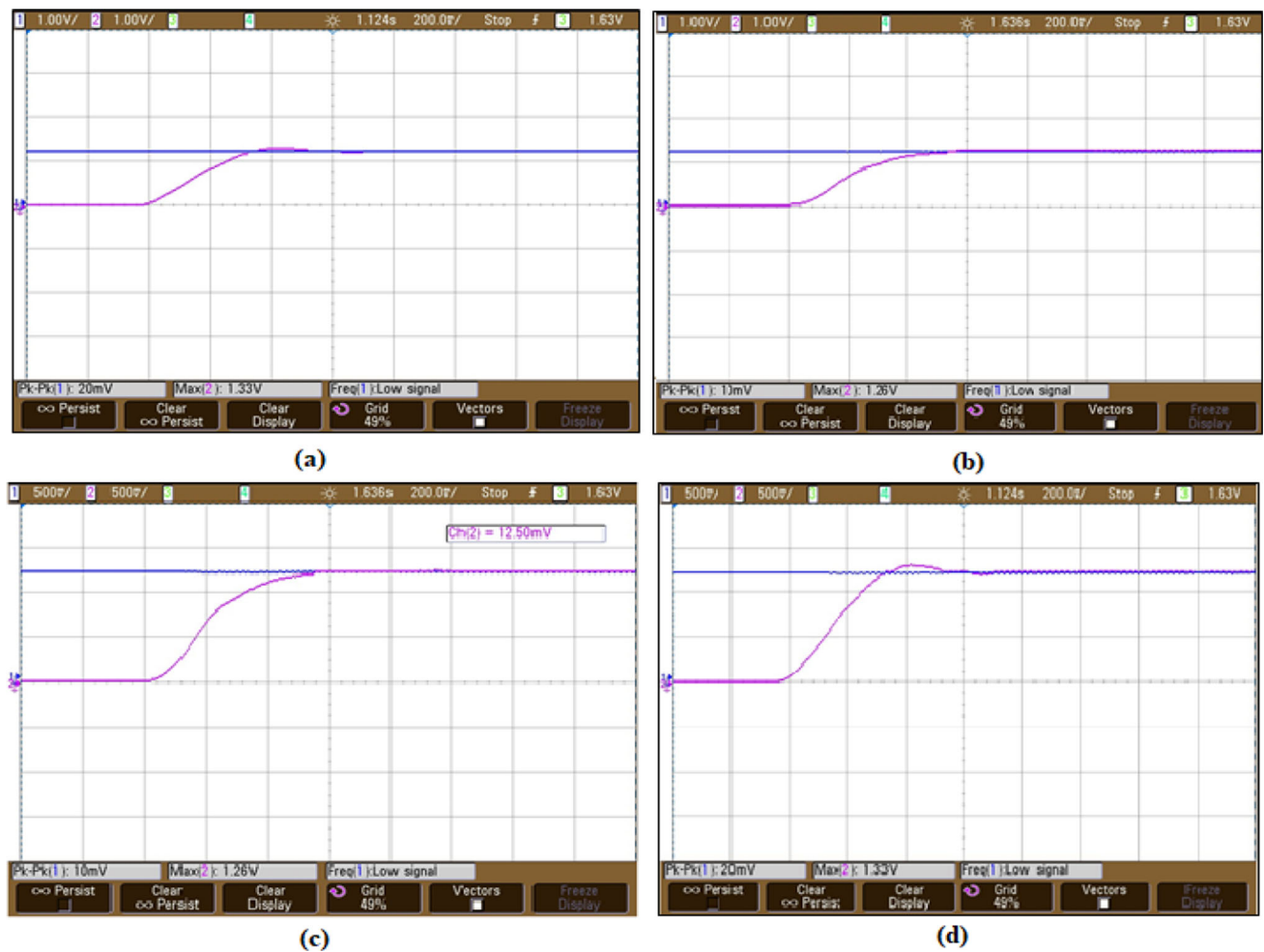


Fig. 24 Speed profile of SRM: a at no load, b with 1NM load, c with 2NM load, and d with 3NM load

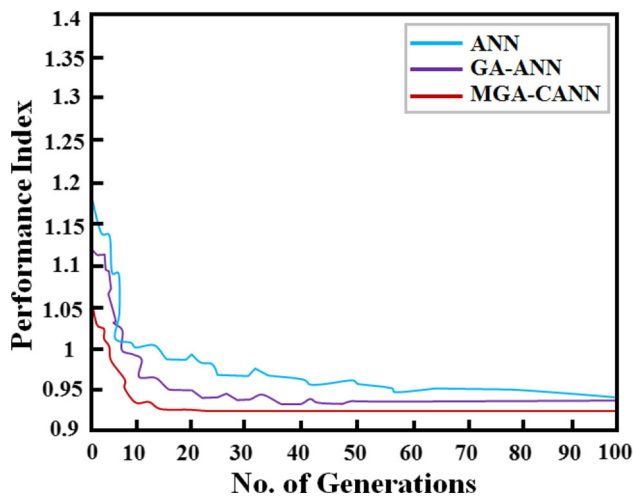


Fig. 25 Convergence curve for controller performance

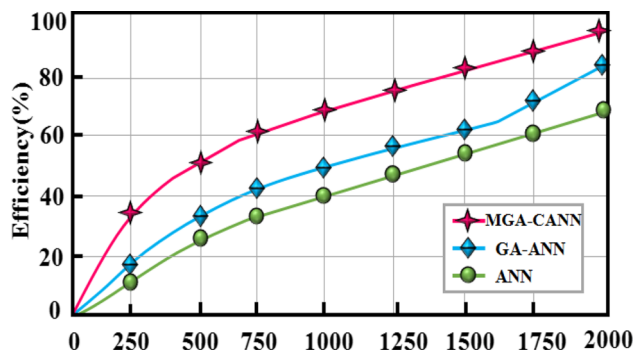


Fig. 26 Comparison of SRM efficiency using intelligent control techniques

achieves a significantly lower torque ripple of 5.2% at 2000 r/min compared to the other methods.

The convergence curve in Fig. 25 illustrates the convergence characteristics of different control techniques, namely artificial neural networks (ANN) and genetic algorithm optimized ANN (GA-ANN), along with the proposed MGA-CANN. The proposed MGA-CANN technique exhibits superior convergence, emphasizing its efficacy in minimizing torque ripples compared to other approaches. The curve showcases the proposed strategy's ability to achieve minimal torque ripple values, highlighting its strength in refining the control process and enhancing the stability and precision of SRM.

The efficiency of SRMs is compared using three intelligent control techniques: ANN, GA-ANN, and the proposed MGA-CANN. The efficiency values for each technique are presented in the Fig. 26, showcasing ANN with a maximum efficiency of 79.2%, GA-ANN with a maximum efficiency of 83.6% and the proposed MGA-CANN with a notably higher efficiency of 90.25%. This comparison highlights the superior performance of the MGA-CANN technique in enhancing

the overall efficiency of SRMs compared to the conventional methods. The increased efficiency implies that the proposed MGA-CANN control strategy marks a notable advancement in intelligent motor control.

5 Conclusion

This research signifies a remarkable leap forward in the domain of sensorless control for SRMs through the utilization of IDTC techniques. The pivotal innovation lies in the integration of a (MGA-CANN controller, effectively eliminating the need for external sensors. This strategic integration not only brings about a significant reduction in costs but also contributes to a noteworthy enhancement in SRM efficiency and responsiveness. The MGA-CANN controller plays a crucial role in achieving precise torque control, maintaining an average torque with minimal oscillations. Comparative analyses against existing control methods underscore the superior performance of the proposed system, showcasing a remarkable reduction in torque ripple (5.2%) and an impressive increase in efficiency 90.25%. This study, thus, stands as a commendable achievement in motor control technology, offering a cost-effective, stable, and efficient solution for SRMs through the incorporation of intelligent control strategies.

Authors' contributions Conceptualization, data curation, and writing-original draft were contributed by NR, Methodology and writing review and editing were involved by KNR and NR, project administration, supervision, and validation were performed by KNR.

Funding The authors received no specific funding for this study.

Availability of data and materials Not applicable.

Declarations

Ethical approval Not applicable.

Conflict of interest An authors have no conflicts of interest to declare that are relevant to the content of this article.

References

1. De Paula MV, dos Santos Barros TA (2021) A sliding mode DITC cruise control for SRM with steepest descent minimum torque ripple point tracking. *IEEE Trans Ind Electron* 69(1):151–159
2. Sun X, Feng L, Diao K, Yang Z (2020) An improved direct instantaneous torque control based on adaptive terminal sliding mode for a segmented-rotor SRM. *IEEE Trans Ind Electron* 68(11):10569–10579
3. Sun X, Wu J, Lei G, Guo Y, Zhu J (2020) Torque ripple reduction of SRM drive using improved direct torque control with sliding mode controller and observer. *IEEE Trans Ind Electron* 68(10):9334–9345

4. Hao Z, Yu Q, Cao X, Deng X, Shen X (2020) An improved direct torque control for a single-winding bearingless switched reluctance motor. *IEEE Trans Energy Convers* 35(3):1381–1393
5. Wang S, Hu Z, Cui X (2020) Research on novel direct instantaneous torque control strategy for switched reluctance motor. *IEEE Access* 8:66910–66916
6. Sun Q, Wu J, Gan C (2020) Optimized direct instantaneous torque control for SRMs with efficiency improvement. *IEEE Trans Ind Electron* 68(3):2072–2082
7. Diao K, Sun X, Lei G, Guo Y, Zhu J (2020) Multiobjective system level optimization method for switched reluctance motor drive systems using finite-element model. *IEEE Trans Ind Electron* 67(12):10055–10064
8. Kimpara ML, Reis RR, Da Silva LE, Pinto JO, Fahimi B (2022) A two-step control approach for torque ripple and vibration reduction in switched reluctance motor drives. *IEEE Access* 10:82106–82118
9. Fang G, Ye J, Xiao D, Xia Z, Wang X, Guo X, Emadi A (2021) An intersection-method-based current controller for switched reluctance machines with robust tracking performance. *IEEE Trans Transp Electrific* 7(4):2822–2834
10. Boler O, Gundogmus O, Sozer Y (2020) Direct voltage controller for SRMs in achieving torque ripple minimization over wide speed range. In *2020 IEEE energy conversion congress and exposition (ECCE)*, pp 4674–4680. IEEE, 2020.
11. Gan C, Chen Y, Sun Q, Si J, Wu J, Hu Y (2020) A position sensorless torque control strategy for switched reluctance machines with fewer current sensors. *IEEE/ASME Trans Mechatron* 26(2):1118–1128
12. Ahmad SS, Narayanan G (2020) Evaluation of dc-link capacitor RMS current in switched reluctance motor drive. *IEEE Trans Ind Appl* 57(2):1459–1471
13. Pupadubsin R, Mecrow BC, Widmer JD, Steven A (2020) Smooth voltage PWM for vibration and acoustic noise reduction in switched reluctance machines. *IEEE Trans Energy Convers* 36(3):1578–1588
14. Sun H, Dou Y, Chen Y (2023) A space vector pulse width modulation method for switched reluctance motor driven by full bridge power converter. *IET Electric Power Appl*.
15. Jing B, Dang X, Liu Z, Long S (2022) Torque ripple suppression of switched reluctance motor based on fuzzy indirect instant torque control. *IEEE Access* 10:75472–75481
16. Tariq I, Muzzammel R, Alqasmi U, Raza A (2020) Artificial neural network-based control of switched reluctance motor for torque ripple reduction. *Math Probl Eng* 2020:1–31
17. Cai Y, Dong Z, Liu H, Liu Y, Wu Y (2023) Direct instantaneous torque control of SRM based on a novel multilevel converter for low torque ripple. *World Electric Vehicle J* 14(6):140
18. Chen X, Zhang Z, Yu L, Bian Z (2020) An improved direct instantaneous torque control of doubly salient electromagnetic machine for torque ripple reduction. *IEEE Trans Ind Electron* 68(8):6481–6492
19. Hamouda M, Al-Amyal F, Odinaev I, Ibrahim MN, Számel L (2022) A novel universal torque control of switched reluctance motors for electric vehicles. *Mathematics* 10(20):3833
20. Al-Amyal F, Számel L, Hamouda M (2023) An enhanced direct instantaneous torque control of switched reluctance motor drives using ant colony optimization. *Ain Shams Eng J* 14(5):101967
21. Reis RR, Kimpara ML, Galotto L, Pinto JO (2023) Genetic algorithm-based commutation angle control for torque ripple mitigation in switched reluctance motor drives. *IEEE Access*
22. Selvi RK, Malar RS (2020) A bridgeless Luo converter based speed control of switched reluctance motor using Particle Swarm Optimization (PSO) tuned proportional integral (Pi) controller. *Microprocess Microsyst* 75:103039
23. Rahman MS, Lukman GF, Hieu PT, Jeong KI, Ahn JW (2021) Optimization and characteristics analysis of high torque density 12/8 switched reluctance motor using metaheuristic gray wolf optimization algorithm. *Energies* 14(7):2013
24. Saha N, Mishra PC (2023) Modified whale algorithm-based optimization for fractional order concurrent diminution of torque ripple in switch reluctance motor for EV applications. *Processes* 11(4):1226
25. Kotb H, Yakout AH, Attia MA, Turky RA, AboRas KM (2022) Speed control and torque ripple minimization of SRM using local unimodal sampling and spotted hyena algorithms based cascaded PID controller. *Ain Shams Eng J* 13(4):101719
26. Fang G, Scalcon FP, Xiao D, Vieira RP, Gründling HA, Emadi A (2021) Advanced control of switched reluctance motors (SRMs): a review on current regulation, torque control and vibration suppression. *IEEE Open J Ind Electron Soc* 2:280–301

Publisher's Note Springer Nature remains neutral with regard to jurisdictional claims in published maps and institutional affiliations.

Springer Nature or its licensor (e.g. a society or other partner) holds exclusive rights to this article under a publishing agreement with the author(s) or other rightsholder(s); author self-archiving of the accepted manuscript version of this article is solely governed by the terms of such publishing agreement and applicable law.